ENGINEERING RESEARCH INSTITUTE
UNIVERSITY OF MICHIGAN
ANN ARBOR

QUARTERLY PROGRESS REPORT NO. 1

August 1, 1953 to December 31, 1953

INTERMITTENT DETONATION AS A THRUST-PRODUCING MECHANISM

By

J. A. NICHOLLS

H. R. WILKINSON

R. B. MORRISON

Project 2172

WRIGHT AERONAUTICAL DIVISION
CURTISS-WRIGHT CORPORATION

January, 1954

ACKNOWLEDGEMENT

Sincere appreciation is extended to Edward J. Schaefer, who assisted by working out the instrumentation and calibration problems associated with the accelerometer measurements.

FOREWORD

The work reported herein was conducted under University of Michigan, Engineering Research Institute Project Number 2172, for the Wright Aeronautical Divisicn of the Curtiss-Wright Corporation. All the work was done by personnel of the Aircraft Propulsion Laboratory.

TABLE OF CONTENTS

LIST OF FIGURES

ABSTRACT

The feasibility of using intermittent detonation as a thrust-producing mechanism is discussed and considered theoretically. The thrust derived from a single detonation wave was measured experimentally by noting the deflection and acceleration of a ballistic pendulum. The acceleration-time traces have yielded valuable information on the pressures and wave processes.

While the impulse predicted by the simplified theory is reasonably close to the experimental impulse, the force-time variation in achieving this impulse is markedly different from that postulated.

INTERMITTENT DETONATION AS A THRUST-PRODUCING MECHANISM

INTRODUCTION

The phenomenon of detonative combustion has been studied extensively in the past by a number of investigators. In general, these investigations were directed toward furthering the understanding of the phenomenon both from the chemical and the hydrodynamic point of view. Such knowledge is, of course, essential to minimizing the dangers of inadvertent detonation and improving the design of explosives. However, very little has been done from the standpoint of harnessing the energy associated with these highly supersonic combustion waves. In recent years some thought has been given to the possibility of stabilizing a detonation wave in a steady-flow thermodynamic cycle. More recently the idea of using intermittent detonation in the manner of a pulse jet has been advanced.*

The work reported here is directed toward ascertaining the possibility of the intermittent-type cycle. On the basis of a simplified, theoretical analysis, which was made earlier, the application appears worthy of further study. These theoretical results predict very high thrusts per unit combustion-chamber area, although the specific impulse is rather low. The physical mechanism for fuel injection, heat exchange, etc., could appreciably alter these predictions in an actual engine.

In this approach to the problem the philosophy has been first to establish experimentally some representative thrusts and impulses derived from a single detonation wave and then to investigate the more prominent parameters affecting these results. On the basis of these initial findings an attempt will be made to achieve cyclic detonation in a tube or series of tubes.

---

* A literature search is currently in progress to consolidate existing information on the possibilities of detonative combustion engines.

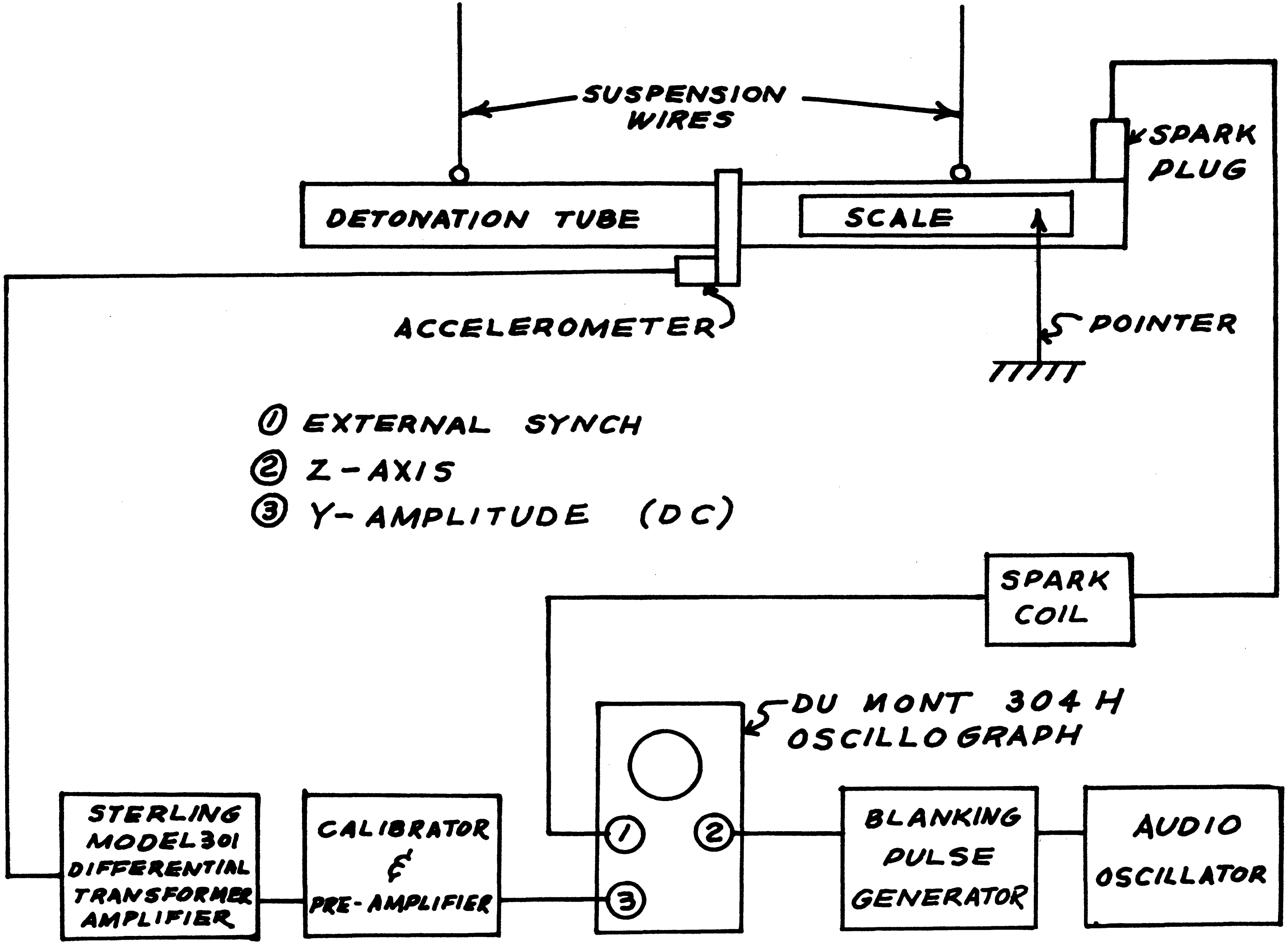

FIG. 10 – BLOCK DIAGRAM OF INSTRUMENTATION

PRESSURE AND TEMPERATURE RATIOS

ACROSS A DETONATION WAVE

The dynamic properties of a detonation wave are treated quite extensively in reference 2. However, for the sake of continuity, the pertinent relations will be derived here.

A detonation wave in a constant-area duct may be treated as a flow discontinuity with heat addition. Assuming that the discontinuity is stationary, this system may be described by the following equations (see Fig. 1) Condition (1) refers to the unburned gases, while state (2) refers to the conditions after the heat release has been realized.

Conservation of Momentum:

$$P_1 + \rho_1 u_1^2 = P_2 + \rho_2 u_2^2 , \qquad (1)$$

Conservation of Mass:

$$\rho_1 u_1 = \rho_2 u_2 , \qquad (2)$$

Equation of State:

$$P = \rho \frac{R}{m} T , \qquad (3)$$

where

P = static pressure,

ρ = density,

u = velocity,

m = molecular weight,

R = universal gas constant, and

T = static temperature.

Rearranging the momentum equation and introducing the state equation, we may write:

$$P_1 \left[1 + \frac{u_1^2}{R_1 T_1}\right] = P_2 \left[1 + \frac{u_2^2}{R_2 T_2}\right]$$

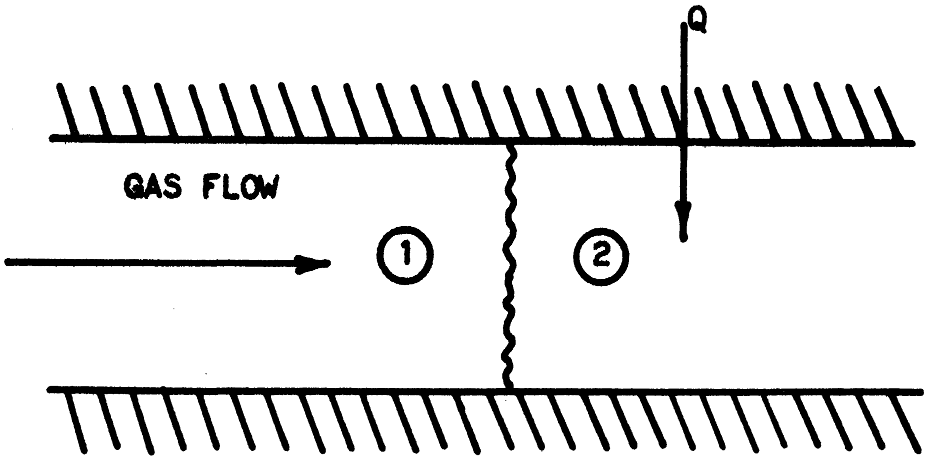

FIG. 1 — DETONATION WAVE IN A CONSTANT-AREA DUCT

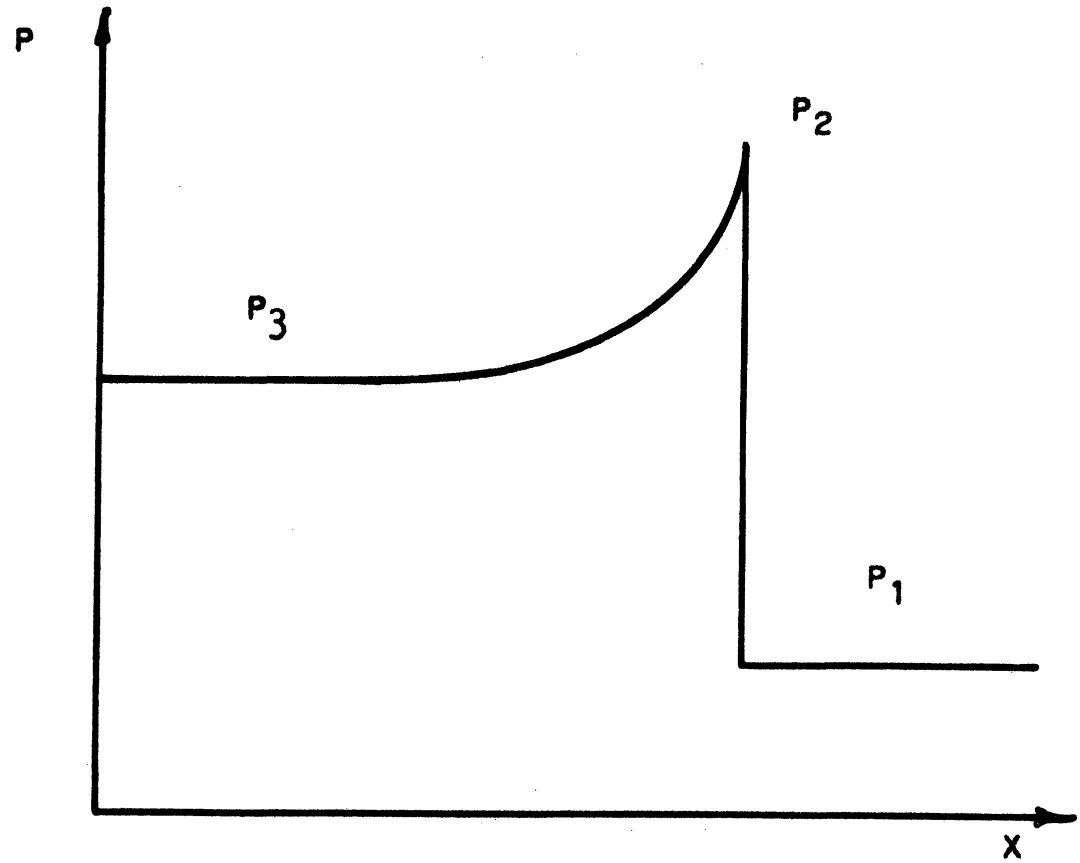

FIG. 2 — PRESSURE DISTRIBUTION ACROSS A DETONATION WAVE

or

$$\frac{P_2}{P_1} = \frac{1 + \gamma_1 M_1^2}{1 + \gamma_2 M_2^2} ,$$

where

γ = ratio of specific heats,

M_1 = Mach number of detonation, and

M_2 = Mach number of the burned gases relative to the front.

In the normal case, detonation is of the Chapman-Jouguet type in which M_2 is unity. The pressure ratio then becomes

$$\frac{P_2}{P_1} = \frac{1 + \gamma_1 M_1^2}{1 + \gamma_2} . \qquad (4)$$

In the case of a flame tube, the pressure established behind the detonation wave, as indicated by equation (4), will be modified by a trailing rarefaction wave. The pressure, P_2, will be reduced to a new plateau value of P_3. A typical pressure distribution for a detonation wave in a flame tube is shown in Fig 2. This plateau pressure is related to the peak pressure by the relation[2]

$$\frac{P_3}{P_1} = \frac{P_2}{P_1} [1 - \frac{\gamma_2 - 1}{2} M_{2c}]^{2\gamma_2/(\gamma_2 - 1)} \qquad (5)$$

where

M_{2c} = Mach number of the burned gases relative to a fixed point on the flame tube,

or

$$\frac{P_3}{P_1} = \left[\frac{1 + \gamma_1 M_1^2}{1 + \gamma_2}\right] \left[1 - \frac{\gamma_2 - 1}{2} M_{2c}\right]^{2\gamma_2/(\gamma_2 - 1)} \qquad (6)$$

In order to derive a relation for the temperature ratio, we may write from the equation of state

$$\frac{T_2}{T_1} = \frac{P_2}{P_1} \cdot \frac{m_2}{m_1} \cdot \frac{\rho_1}{\rho_2} . \qquad (7)$$

Equations (1) and (2) may be readily combined to give

$$(\rho_1 u_1)^2 = (\rho_2 u_2)^2 = \frac{P_1 - P_2}{\frac{1}{\rho_2} - \frac{1}{\rho_1}}$$

$$\rho_1^2 u_1^2 = \frac{\left[1 - \left(\frac{P_2}{P_1}\right)\right] P_1 \rho_1}{\left(\frac{\rho_1}{\rho_2} - 1\right)}$$

or

$$\gamma_1 M_1^2 = \frac{(1 - P_2/P_1)}{(\rho_1/\rho_2 - 1)} .$$

Solving for $\frac{\rho_1}{\rho_2}$ we have

$$\frac{\rho_1}{\rho_2} = \frac{1 - P_2/P_1}{\gamma_1 M_1^2} + 1 . \qquad (8)$$

Introducing (4) and (8) into (7) and simplifying yields

$$T_2/T_1 = \frac{m_2}{m_1} \frac{\gamma_2}{\gamma_1} \frac{1}{M_1^2} \left[\frac{1 + \gamma_1 M_1^2}{1 + \gamma_2}\right]^2 \qquad (9)$$

A plot of the pressure, temperature, density, and molecular-weight ratios for hydrogen-oxygen detonations is shown in Fig. 3. For these calculations the experimental Mach number of detonation as obtained in reference 2 was used. The molecular-weight ratio is based on no dissociation, while the ratio of specific heats in the burned gases was assumed to be 1.15.

THEORETICAL IMPULSE FROM A SINGLE DETONATION WAVE

The relatively high pressures associated with detonative combustion could conceivably be utilized in a jet propulsion device. If such an application is considered on the basis of steady flow, there will be a marked increase in entropy across the wave and the system might appear to be inefficient. However, a standing or stabilized detonation wave has never been attained experimentally; hence the case of cyclic or intermittent detonation will be considered.

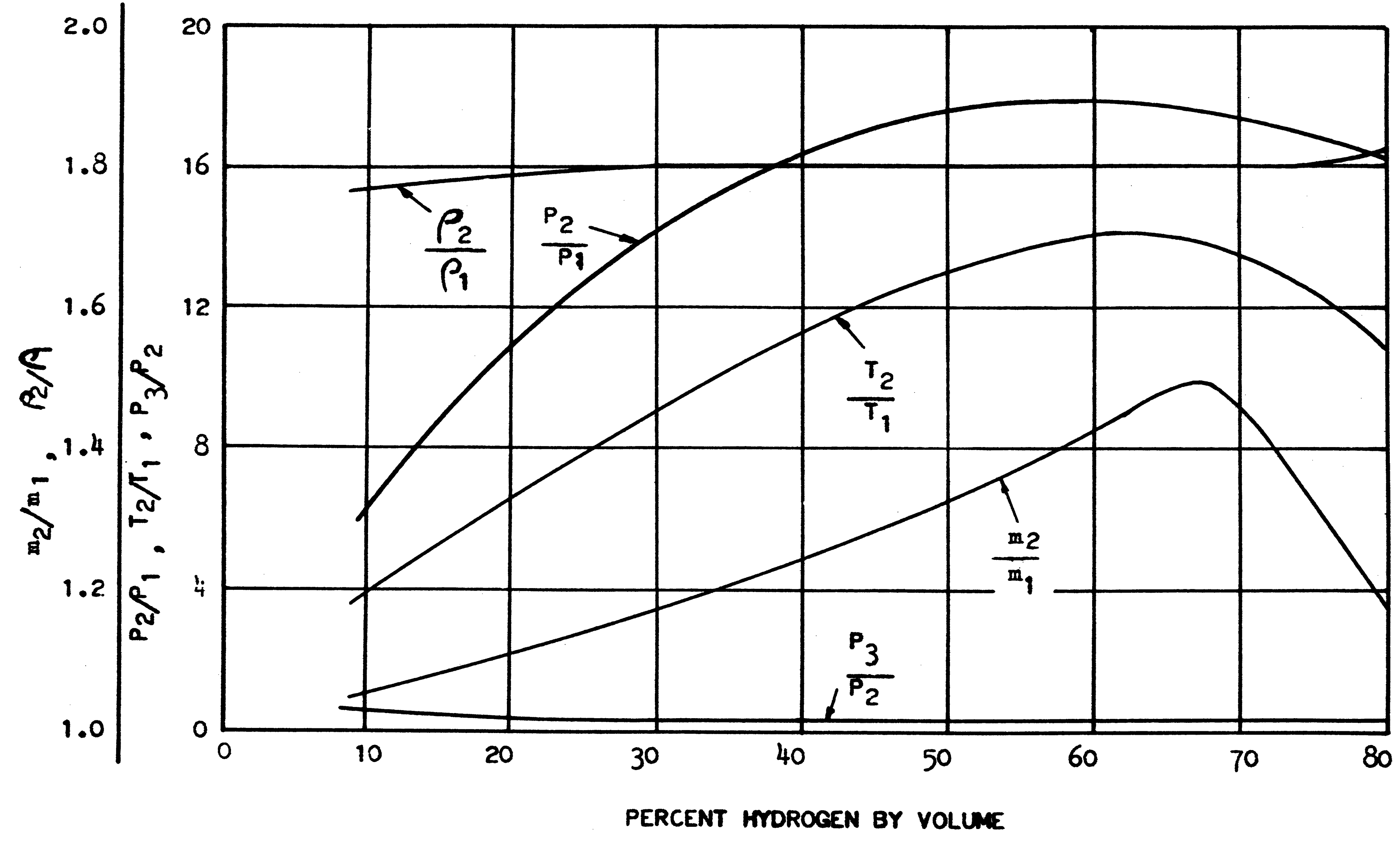

FIG. 3 - THERMODYNAMIC RATIOS ACROSS HYDROGEN-OXYGEN DETONATIONS

Preliminary calculations on an intermittent detonation cycle have been made in reference 1. The theoretical model for those calculations will be used here in evaluating the thrust and impulse that would be expected from a single detonation wave.

Figure 4 represents a detonation tube of length L and cross-sectional area A. The tube is filled with combustible gas and then spark-ignited at the closed end. The flame front will be preceded by a shock wave which is continuously strengthened by the accelerating flame front until detonation is established. At the open end of the tube a rarefaction wave will be reflected which will move through the gases at the local sonic speed. At the closed end of the tube the pressure will gradually be reduced and another rarefaction reflected. These reflections continue but, of course, are gradually damped out.

These detailed processes do not lend themselves to easy quantitative evaluation. Consequently, a few simplifying assumptions will be made. First, it will be assumed that detonation is established immediately and is of the Chapman-Jouguet type. This assumption is somewhat optimistic, although the use of a long tube will tend to minimize the error. The plateau pressure will act on the closed end of the tube until the reflected rarefaction returns. It will also be assumed that the rarefaction returns at the sonic velocity corresponding to state 2 and that it returns as a discontinuity and reduces the pressure to atmospheric. These assumptions are on the conservative side, as they tend to lower the effective time of the thrust force. The subsequent reflected waves will be neglected.

Accordingly, the simplified thrust-time history of a single detonation wave is as shown in Fig. 5. In this figure t_d represents the time for the detonation wave to travel the distance L and t_r the time for the rarefaction to return.

The impulse I may then be expressed as

$$I = \int_0^{t_d + t_r} T\, dt = T\,(t_d + t_r)\ . \qquad (10)$$

Referring to the nomenclature in Fig. 2, the thrust can be evaluated by the pressure differential acting on the head end of the tube, or

$$T = (P_3 - P_1)\, A\ ,$$

where we will assume that the tube is initially filled to the ambient pressure, P_1. Then

$$T = \left(\frac{P_3}{P_1} - 1\right) P_1\, A = P_1\, A \left[\left(\frac{1 + \gamma_1 M_1^2}{1 + \gamma_2}\right)\left(1 - \frac{\gamma_2 - 1}{2} M_{2c}\right)^{2\gamma_2/(\gamma_2 - 1)} - 1\right]$$

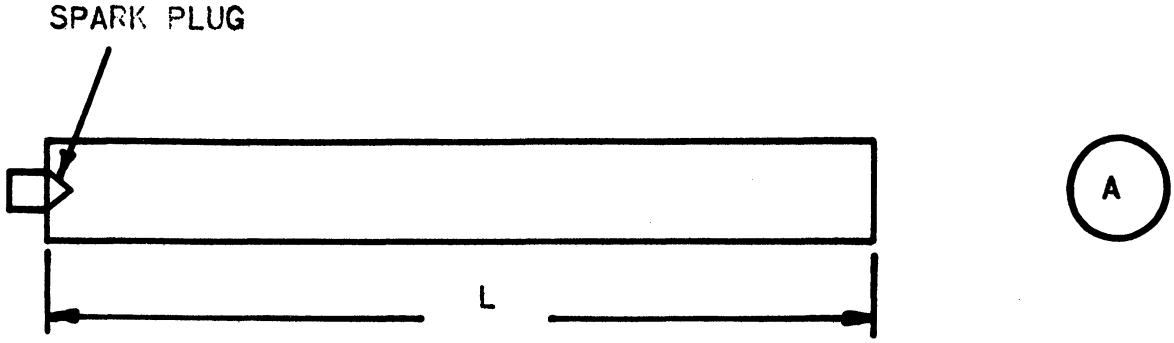

FIG. 4 — DETONATION TUBE

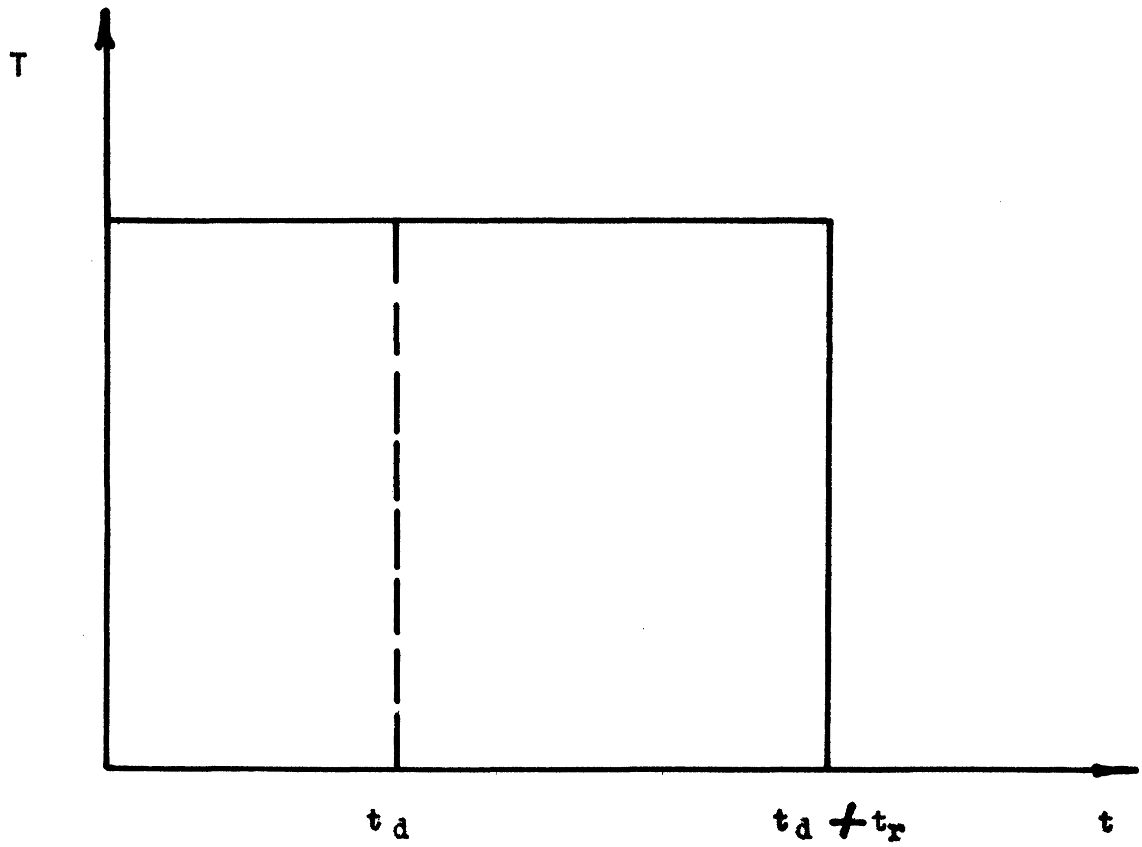

FIG. 5 — IDEALIZED THRUST-TIME HISTORY
OF A SINGLE DETONATION WAVE

Further

$$t_d = \frac{L}{V_d} = \frac{L}{V_1}$$

and $t_r = \frac{L}{V_r} = \frac{L}{V_2} = \frac{L}{\sqrt{\gamma_2 R_2 T_2}}$,

where

V_d = velocity of detonation wave and

V_r = velocity of rarefaction wave.

Finally,

$$I = P_1 A L \left[\left(\frac{1+\gamma_1 M_1{}^2}{1+\gamma_2} \right) \left(1 - \frac{\gamma_2 - 1}{2} M_{2c} \right)^{2\gamma_2/(\gamma_2-1)} - 1 \right] \left[\frac{1}{V_d} + \frac{1}{\sqrt{\gamma_2 R_2 T_2}} \right] \quad (11)$$

The specific impulse I_s or the ratio of impulse to the weight of fuel, may be written as

$$I_s = \frac{I}{w_f} .$$

If oxygen is used as the oxidant rather than air, the propulsion system is penalized for the additional weight of the oxygen; hence

$$I_s = \frac{I}{w_f + w_{O2}} ,$$

where

w_f = weight of fuel and

w_{O2} = weight of oxygen.

Then

$$w_f = \rho_f \, f \, A \, L$$

and

$$w_{O2} = \rho_{O2} \, A \, L \, (1 - f)$$

where

f = percent by volume of fuel and
A L = volume of tube.

Then

$$I_s = \frac{P_1 \left[\left(\frac{1+\gamma_1 M_1^2}{1+\gamma_2}\right)\left(1-\frac{\gamma_2-1}{2} M_{2c}\right)^{2\gamma_2/(\gamma_2-1)} - 1\right]\left[\frac{1}{V_d} + \frac{1}{\sqrt{\gamma_2 R_2 T_2}}\right]}{f \rho_f + (1-f)\rho_{o2}} \qquad (12)$$

The thrust, impulse, or specific impulse may now be evaluated from these equations. The values of V_d are available from previous experiments[2]. However, it is necessary to assume a value of γ_2.

As with other propulsive systems, the geometry does not enter into the specific impulse. Contrary to other systems, however, the impulse is directly proportional to the length.

EXPERIMENTAL DETERMINATION OF THE IMPULSE FROM A SINGLE DETONATION WAVE

The theory developed is subject to modification in the real case where detonation does not ensue immediately and where unsteady fluid flow replaces the simple wave processes assumed. To gain some insight into the magnitude of these discrepancies, the impulses were determined experimentally and compared with the theory. The experimental arrangement is shown in Fig. 6.

The particular combustible mixture tested was premixed in a stainless-steel reservoir. The reservoir was first evacuated to a pressure of about 0.1 inch of mercury by means of a Cenco Megavac. The fuel and oxidant were then mixed on a partial-pressure basis in which the effects of compressibility were small enough to be neglected. For each run the fuel was blown through the detonation tube. After sufficient purging the downstream end was sealed with a paper diaphragm to prevent diffusion of the test gases into the air. The pet cock was closed and the fuel line disconnected. Ordinarily, the mixture was ignited by a conventional automotive-type spark plug, although a glow plug was used on occasion.

To facilitate the measurement of impulse, the detonation tube was suspended from the ceiling as a ballistic pendulum. Two pieces of 1/16-inch-diameter stainless-steel aircraft cable, 12.5 feet in length, served as the suspension.

Two different detonation tubes were utilized in order to obtain reasonable deflections and accelerations for the different gaseous mixtures

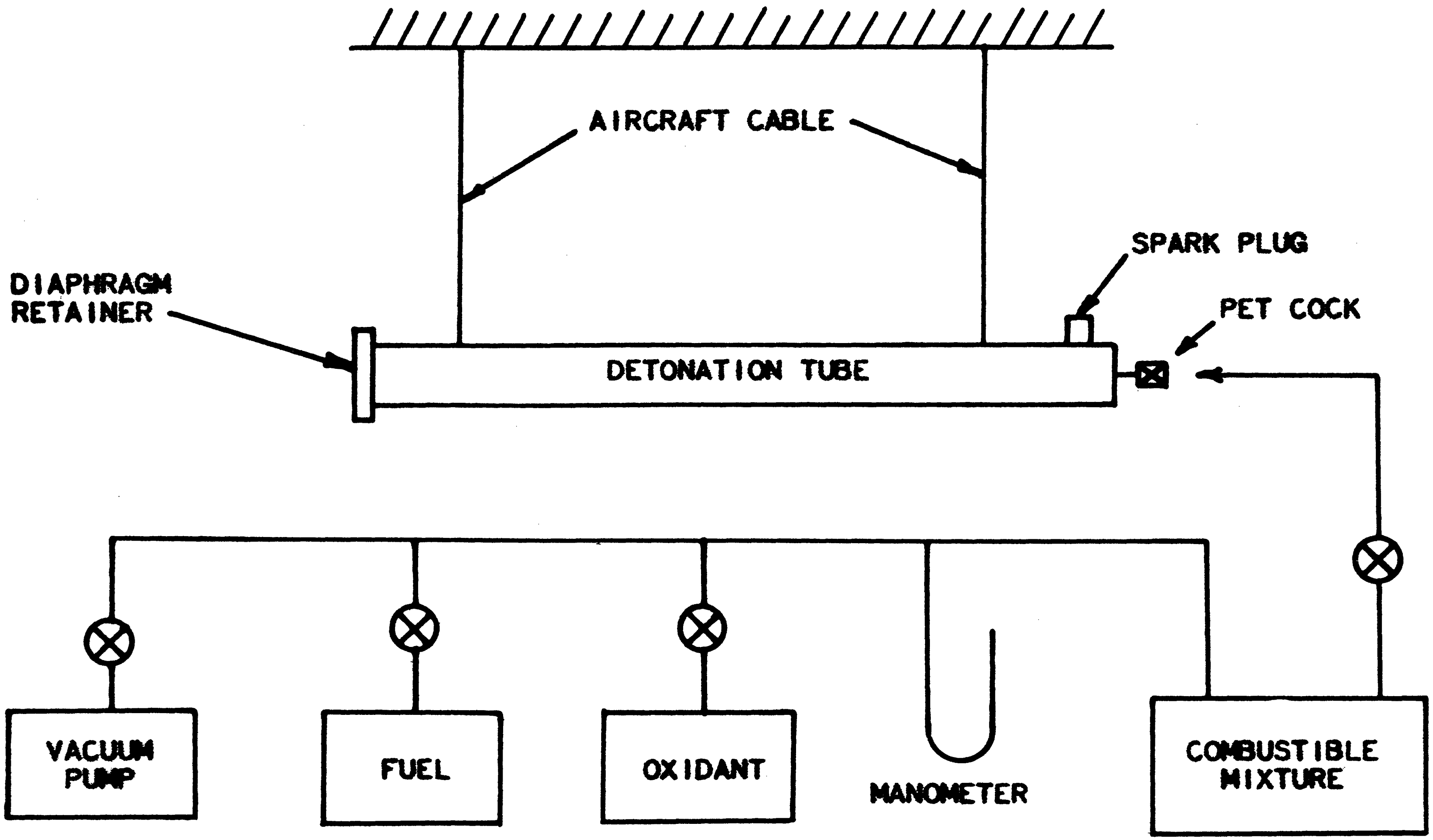

FIG. 6 - EXPERIMENTAL ARRANGEMENT

used. These tubes will be designated as tube A and tube B and are shown in Fig. 7.

The experimental measurements of impulse were made by two different methods, and will be discussed separately.

DEFLECTION OF A BALLISTIC PENDULUM

The first method used in evaluating the impulse of a single detonation wave was based on the impulse-momentum relation. That is,

$$I = \int F \, dt = \frac{W}{g} V ,$$

where

W = weight of tube and

V = maximum velocity of tube.

As the tube is fired the thrust force causes it to swing in an arc, converting the kinetic energy into potential energy. If it is assumed that the tube achieves its kinetic energy without a change in elevation (and this assumption is well within the limits of experimental accuracy), the energy balance can be written as

$$\frac{1}{2} \frac{W}{g} V^2 = W h = W (1 - b \cot \theta)$$

or

$$I = W \sqrt{\frac{2}{g} (1 - b \cot \theta)} , \qquad (13)$$

where $\theta = \sin^{-1} \frac{b}{l}$ and the nomenclature is as shown in Fig. 8.

A plot of equation (13) is included as Fig. 9

The experimental procedure consisted simply of noting the deflection, b, for each detonation. This measurement was accomplished by superimposing a scale on the side of the tube and then noting visually the movement of the scale past a fixed vertical reference line.

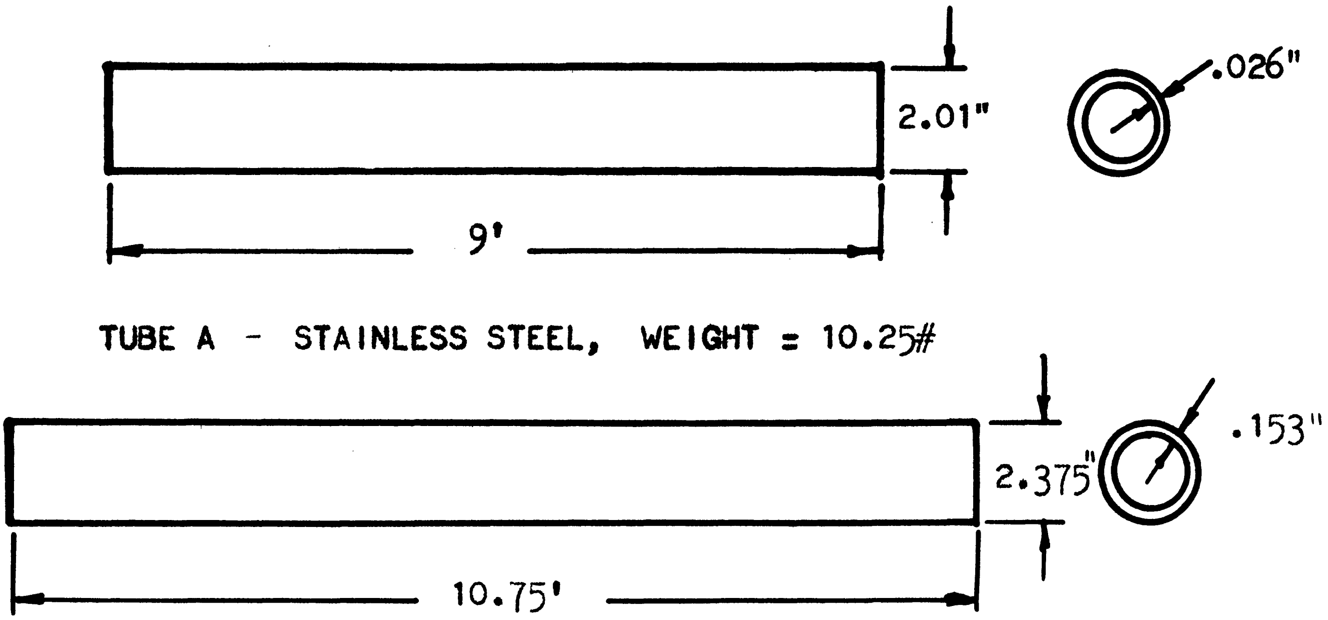

TUBE A - STAINLESS STEEL, WEIGHT = 10.25#

TUBE B - BRASS, WEIGHT = 48.5#

FIG. 7 - DETONATION TUBES

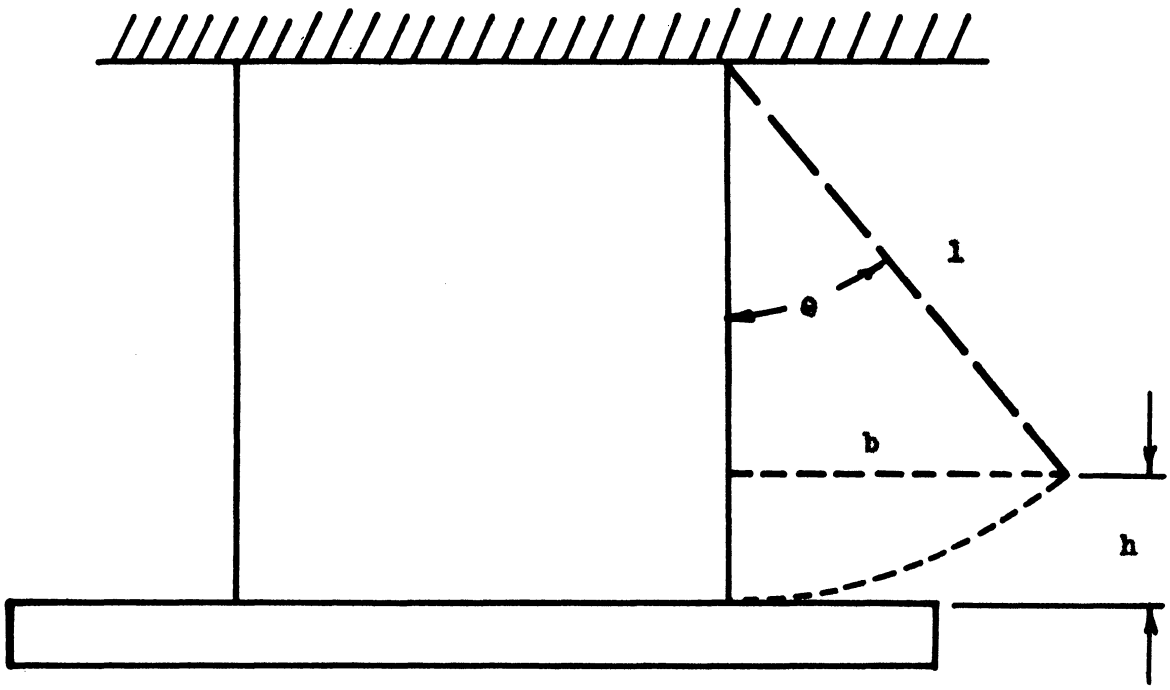

FIG. 8 - GEOMETRY FOR DEFLECTION CALCULATIONS

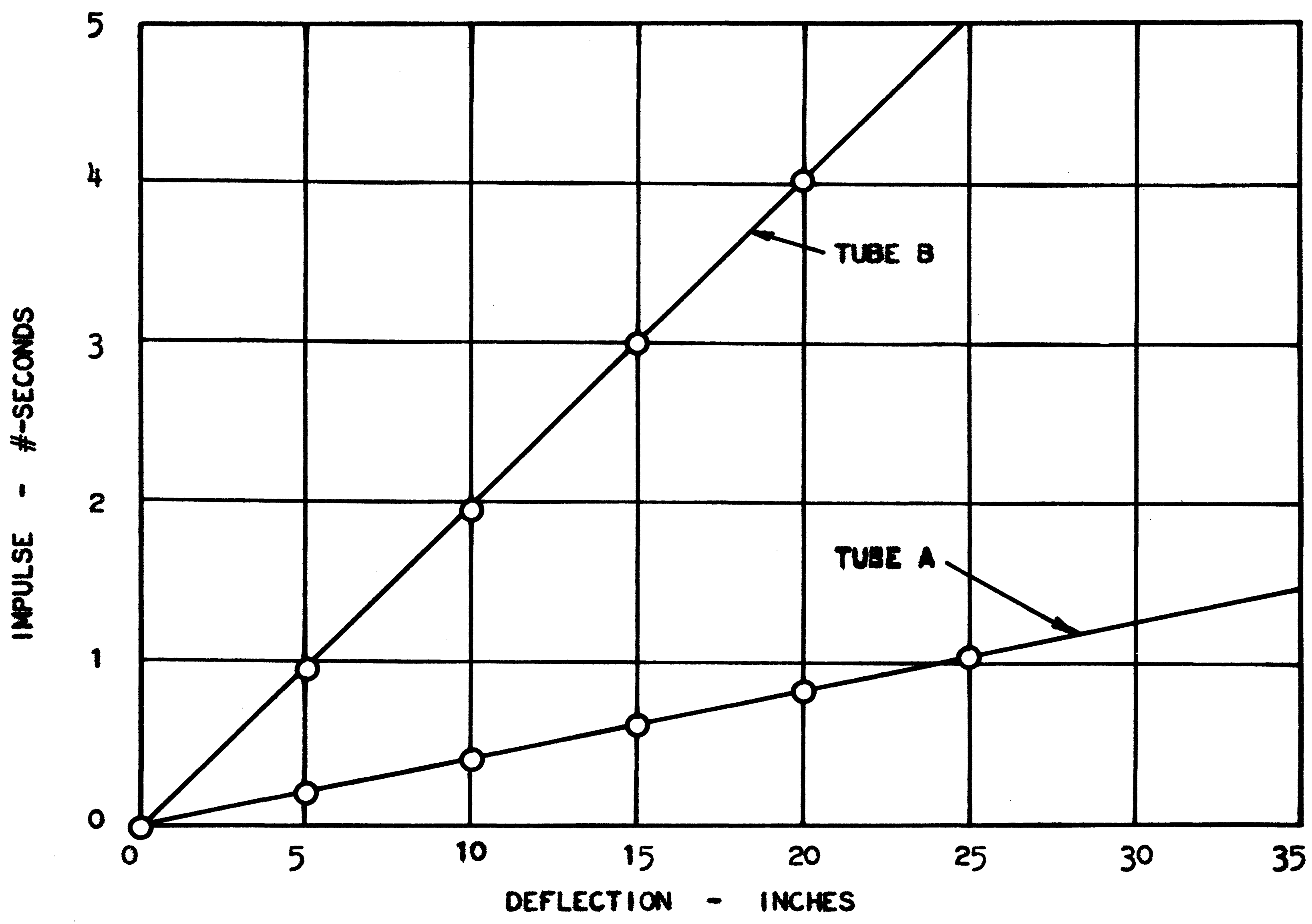

FIG. 9 — CURVE OF IMPULSE VS. DEFLECTION

ACCELEROMETER MEASUREMENTS

Although the deflection method afforded a convenient means of measuring the impulse, it yielded no information as to the variation of thrust with time. Such information would be extremely pertinent to the design of an intermittent detonating device. Accordingly, an accelerometer was mounted at the center of the tube so that the variation of tube acceleration (and hence thrust and pressure) with time could be obtained. The schematic arrangement for making these measurements is shown in Fig. 10. The instrumentation and calibration equipment associated with the accelerometer traces are described in the appendix.

Figure 11 is a photograph of the brass detonation tube, while Fig. 12 is a photograph of the instrumentation.

RESULTS AND DISCUSSION

A series of runs were made with hydrogen-oxygen mixtures in tube A. For these runs the impulse was obtained by the deflection method and is plotted in Fig. 13 as a function of the mixture ratio. The specific impulse, or the impulse divided by the weight of the hydrogen and oxygen, is also shown on this curve and is compared with the theoretical values. As may be seen, the agreement is quite good with richer mixtures, but there is a radical departure as the mixture is leaned below 45 percent. This mixture ratio checks very well with spark-schlieren photographs of hydrogen-oxygen detonations[3], where two regimes of detonation might be indicated. With mixtures below about 45 percent, the initial shock front of the detonation is followed by an array of oblique shock waves and then the lagging combustion. The burning phase lags more and more as the mixture becomes leaner. However, in the case of mixture ratios greater than 45 percent, the detonation is relatively clean, with the combustion evidently initiated right in the shock front. It appears reasonable that the leaner unstable mixtures (possibly subject to spinning detonation) are less prone to detonate, which would account for the defect in the impulse.

The specific impulse of the hydrogen-oxygen mixtures is quite low and is seen to increase with the richer mixtures even though the impulse is falling off. The low values are, of course, attributable to the oxygen, which is included in the specific impulse; but the increase in hydrogen decreases the weight of the fuel-oxygen mixture sufficiently to overbalance

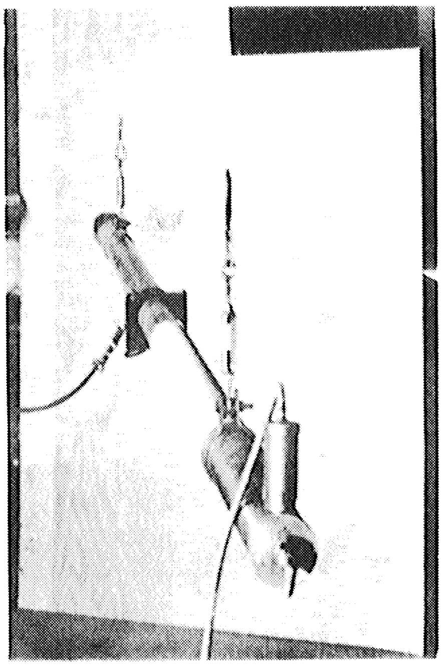

Fig. 11. Photograph of Detonation Tube B.

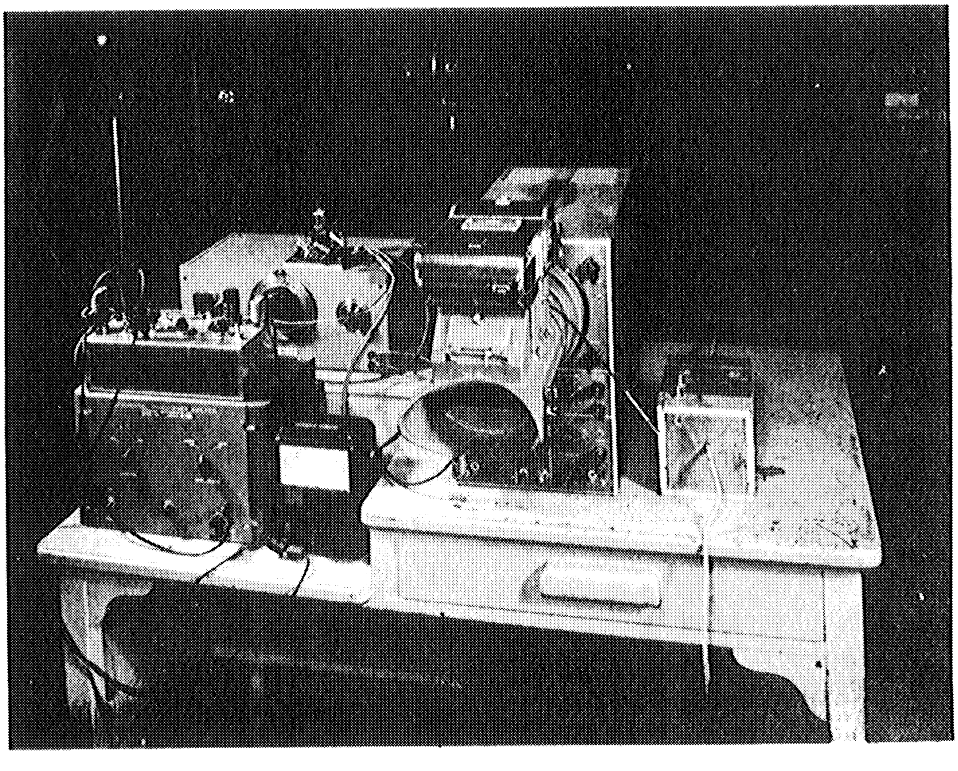

Fig. 12. Photograph of Accelerometer Instrumentation.

the decreasing impulse. In the case of hydrogen-air mixtures, the specific impulse should be materially improved.

In Fig. 14 is shown the impulse and specific impulse of acetylene-oxygen mixtures in which the deflection was also measured. The detonations were initiated by a glow plug. There was appreciable scatter in the experimental points for the lean and rich mixtures, but the results were quite consistent for mixtures in the neighborhood of 50 percent. It is felt that the glow plug has some effect on this scatter, as it does represent a minimum energy input for the initiation. The maximum impulse was noted at 50 percent, which corresponds to the point of the maximum Mach number of detonation. In the past this mixture ratio has been noted to be one of the easiest to detonate. The specific impulse has been plotted on the basis of the arithmetic average of the points for the impulse curve. The discrepancy between experiment and theory is now appreciable for the lean and rich mixtures. The reasons for this discrepancy will be considered shortly. The chemical considerations involved in the theoretical curve are discussed in reference 4, in which the authors evaluated the equilibrium temperatures and compositions behind acetylene-oxygen detonations.

In another series of runs, made with acetylene-oxygen mixtures in tube B, both the deflection and acceleration were noted. For these runs a conventional spark plug was used. A typical acceleration-time photograph is shown in Fig. 15. The superimposed horizontal lines are calibration lines, while the zero axis is the second line from the top. Time increases to the right and acceleration increases positively downward. The horizontal sweep of the oscillograph was triggered by the spark plug, so that the time lag before establishment of detonation is indicated. Each blanked spot on the zero trace represents 1 millisecond. The fluctuations in the trace are due to longitudinal vibrations set up in the wall of the detonation tube. With the accelerometer mounted at the center of the tube, the frequency detected is the second harmonic of the fundamental frequency of about 450 cps. The natural frequency of the accelerometer used for Fig. 15 is 250 cps, which is too low to follow the tube vibrations correctly. However, comparison with traces of a higher-response accelerometer(800 cps) indicates that the first accelerometer is recording the overall acceleration of the tube correctly. If the accelerometer were mounted at either end of the tube, the fundamental frequency would be predominant and the amplitude of the undesirable vibrations would be much more pronounced. More detailed information on the instrumentation appears in the appendix.

The areas under the accelerometer-time traces were integrated by means of a planimeter so that the impulse obtained in this manner could be compared with that by the deflection method. The results of this comparison are shown in Fig. 16. The agreement is quite good, the average difference

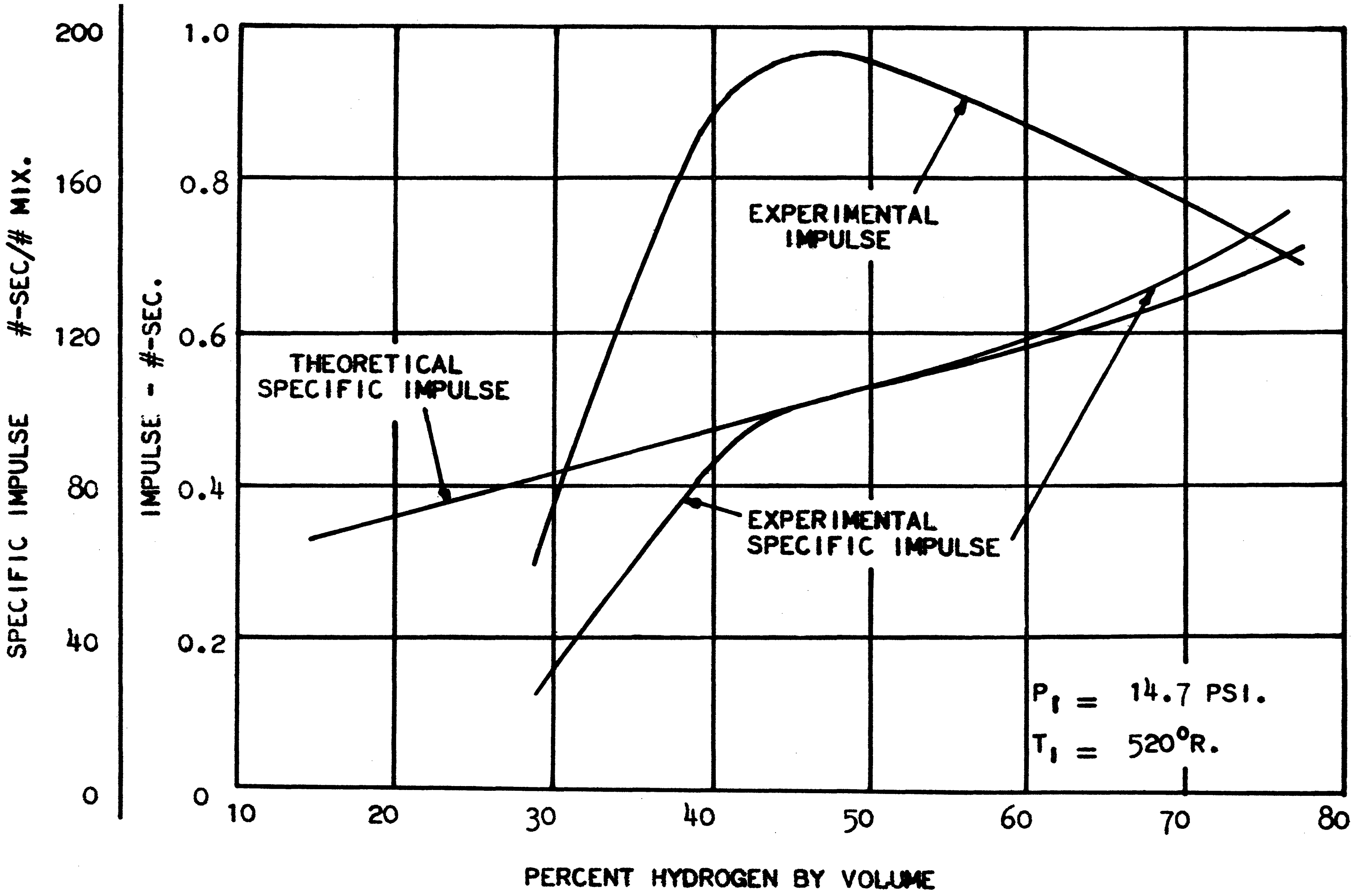

FIG. 13 - IMPULSE DERIVED FROM HYDROGEN - OXYGEN DETONATIONS

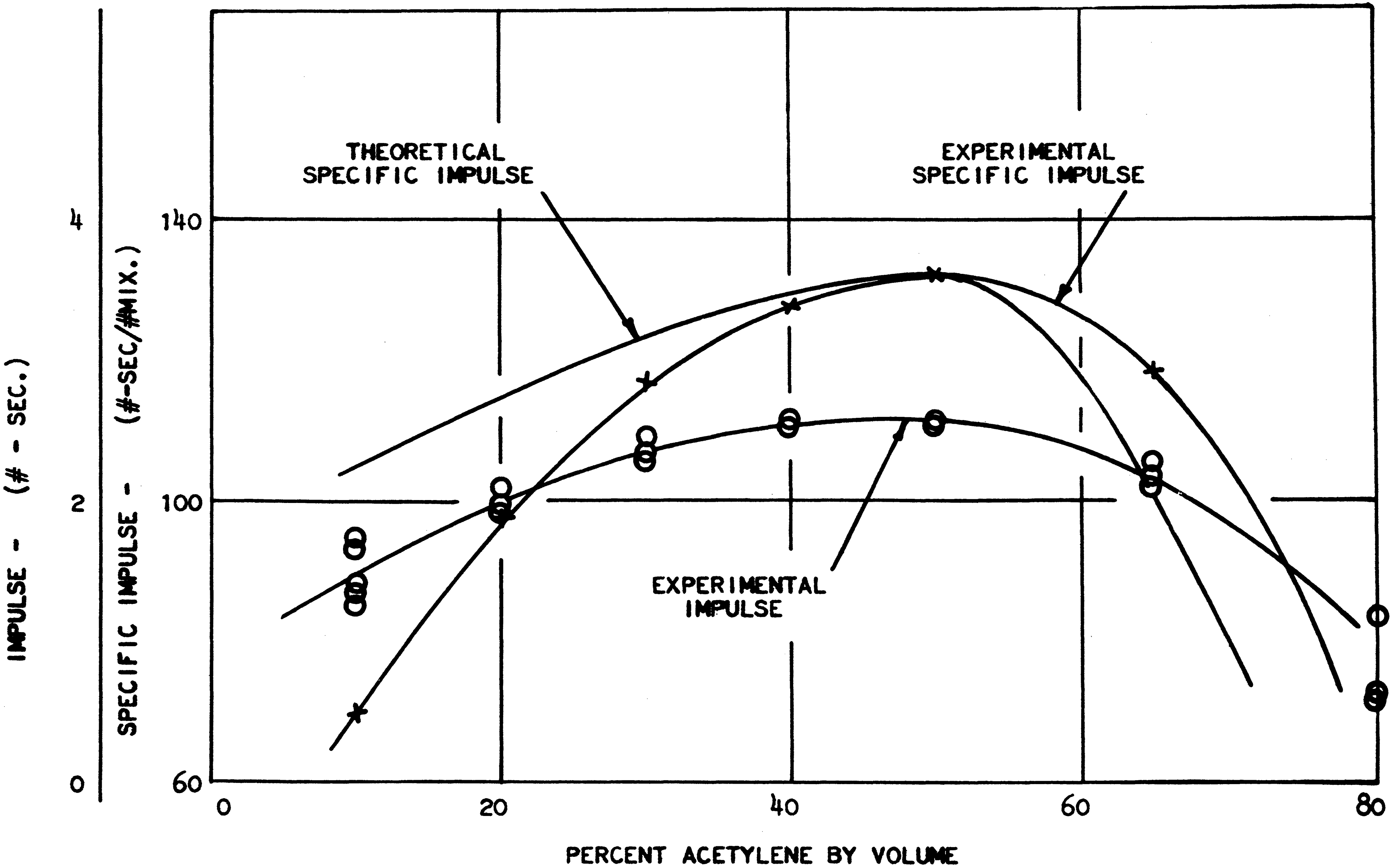

FIG. 14 - IMPULSE DERIVED FROM ACETYLENE-OXYGEN DETONATIONS

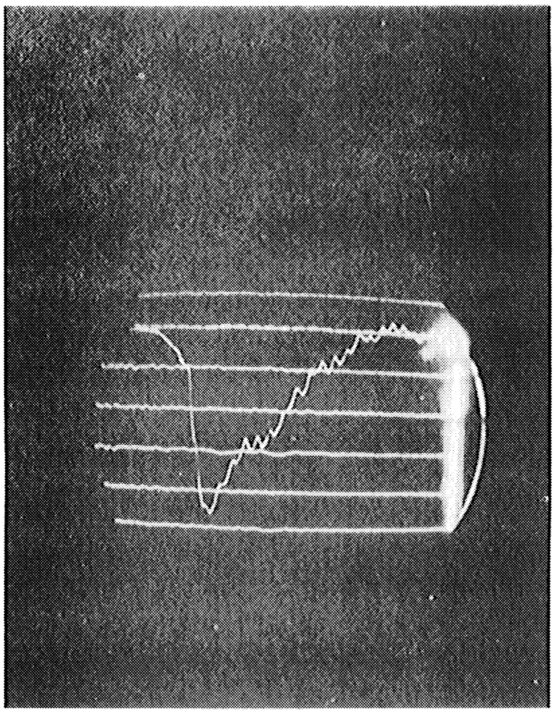

Fig. 15. Acceleration-Time Photograph.

being less than 2 percent. It might be noted that the impulse for this series of runs is somewhat higher than that shown in Fig. 14. The only plausible explanation would seem to lie in the difference of spark plugs. The higher-intensity conventional spark plug undoubtedly initiates detonation sooner than in the case of the glow plug.

The acceleration-time curves for four acetylene-oxygen mixtures are shown in Fig. 17 also included on these curves is the simplified theory. It is interesting that while the theoretical and experimental impulses agree reasonably well, there is a marked difference in the manner of achieving this impulse. As is evident from the traces, the detonation wave is not established instantaneously; rather there is a transient phase, which was described earlier. This transient phase is longer for mixtures near the detonation limits. The shock wave gives rise to a steady increase of pressure on the head end of the tube until the shock strength is sufficient to initiate detonation. The gradual decrease in acceleration (or pressure) is due to the returning rarefaction wave, which is not a discontinuity as was assumed for simplicity. This effect materially lengthens the cycle time, which should be advantageous in the design of a cyclic engine.

The acceleration traces indicate that the tube pressure is reduced to approximately 1/2 atmosphere for a short time. This was observed experimentally,

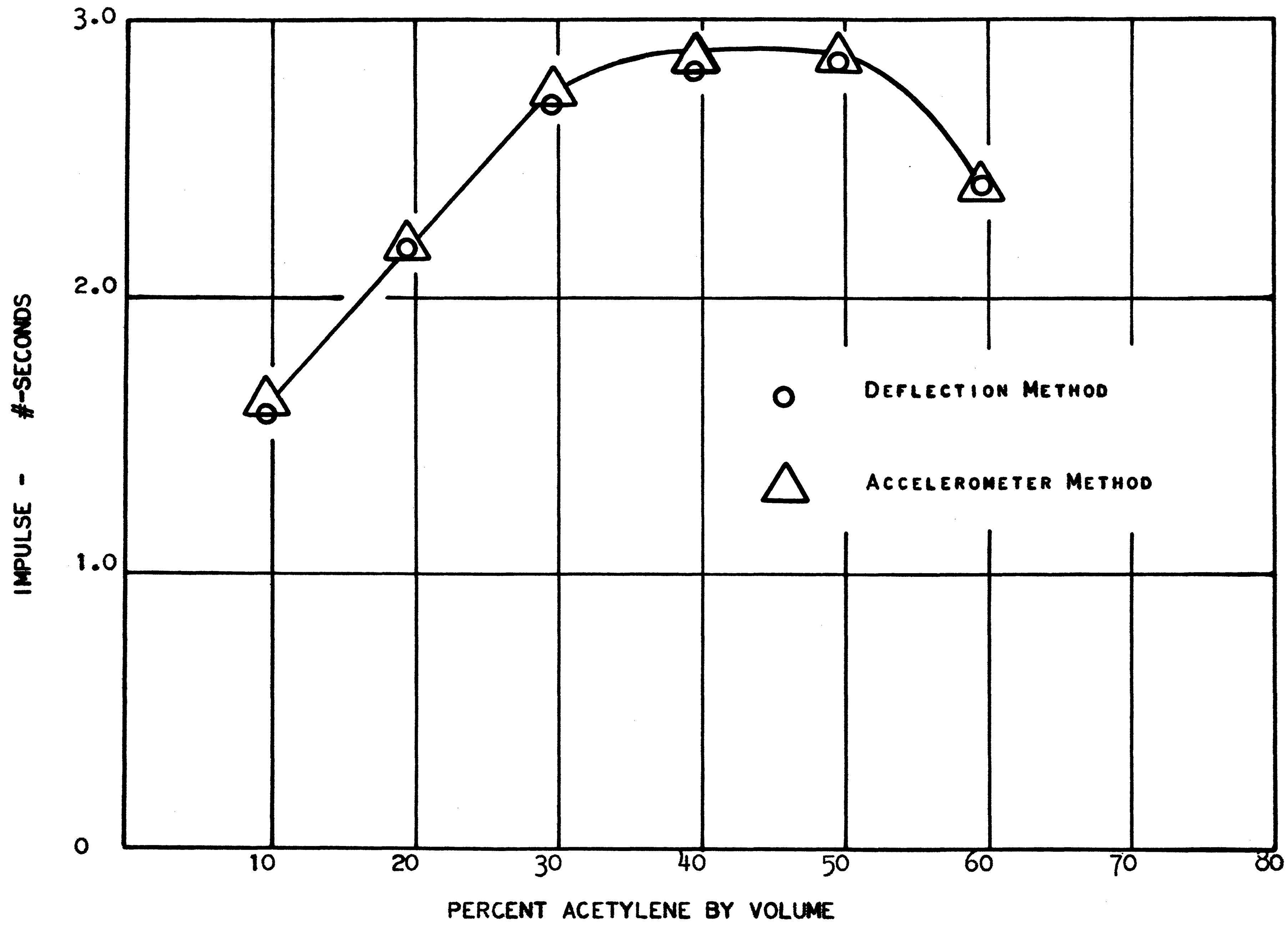

FIG. 16 - COMPARISON OF DEFLECTION AND ACCELEROMETER METHOD

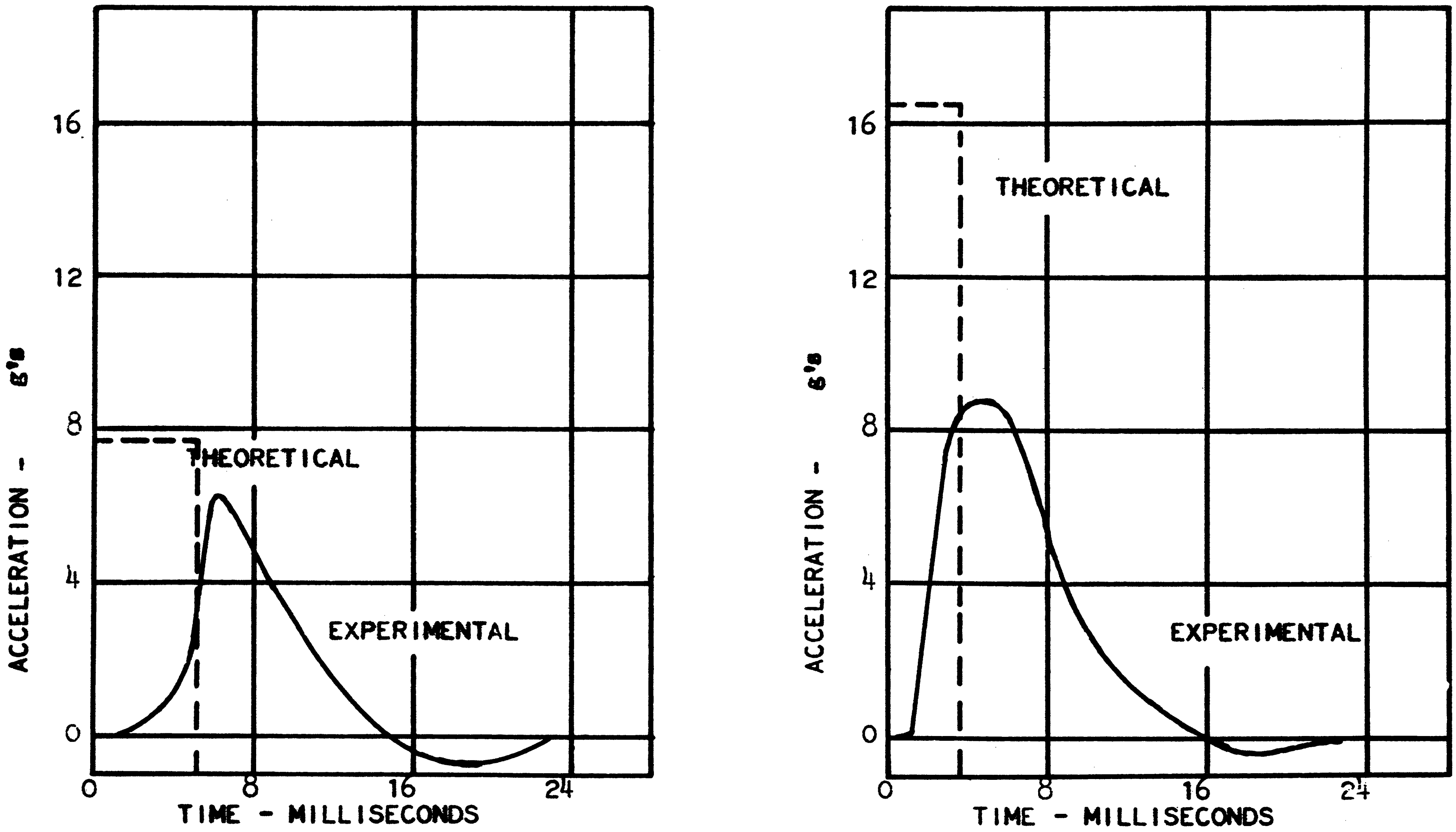

10% ACETYLENE

30% ACETYLENE

FIG. 17 ACCELERATION - TIME GRAPHS OF ACETYLENE-OXYGEN DETONATIONS

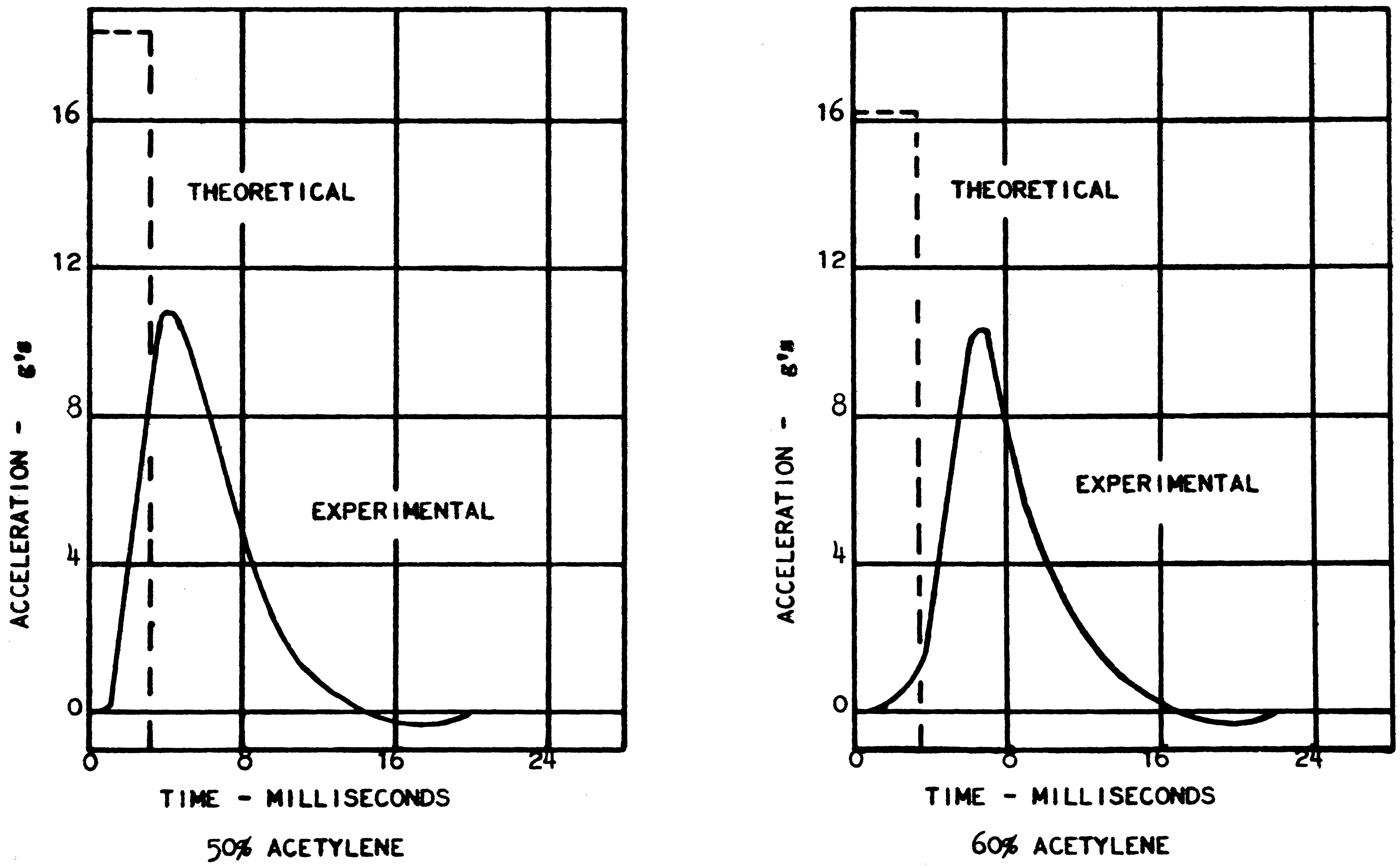

FIG. 17 (CONTINUED) - ACCELERATION - TIME GRAPHS OF ACETYLENE-OXYGEN DETONATIONS

as fragments of the diaphragm were repeatedly found distributed throughout the tube. Conceivably, the reduced pressure could be utilized to induce a fresh charge of fuel.

In operating the detonation tube an appreciable ejector effect was noted at the discharge end. As the exhaust gases were discharged a secondary flow was induced which, in an actual engine, might be worthy of investigation as a device to induce a fresh charge.

FUTURE PLANS

A few more gaseous mixtures will be tested in the detonation tube, especially air mixtures. It is also planned to investigate end effects, that is, the effects of a tail nozzle and different diaphragms.

A literature search is in progress to assimilate existing information on the possibility of utilizing detonation combustion in an engine.

Concurrent with the above studies, thought and effort will be directed toward the design of an intermittent detonative device.

APPENDIX A. INSTRUMENTATION

This section is devoted to a brief description of the equipment shown in block diagram (Fig. 10) with which the acceleration-time history of the impulse detonation tube was obtained.

The acceleration pickup device selected was the Schaevitz type AB accelerometer shown schematically in Fig. 18. The seismic system of this accelerometer consists of a mass suspended by two parallel beryllium-copper

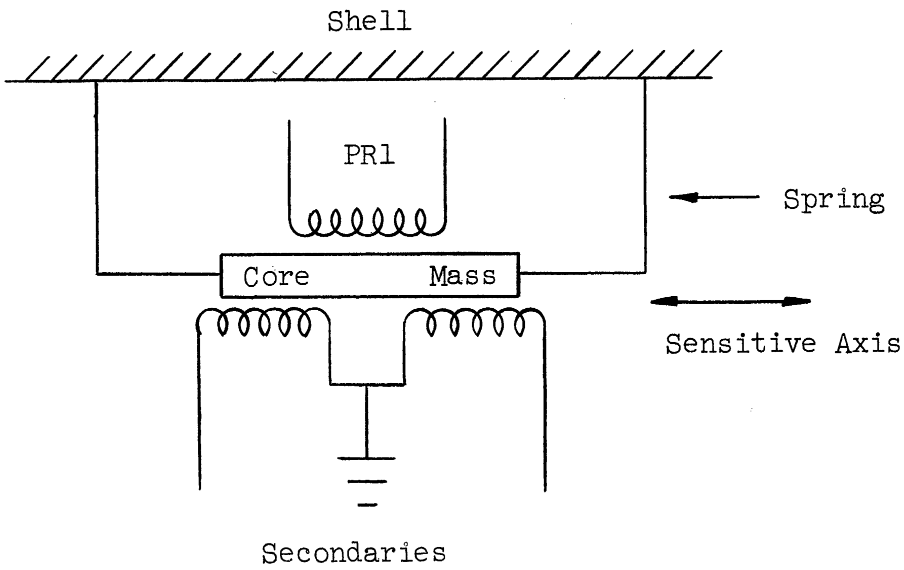

Fig. 18. Linear Accelerometer.

cantilever springs. The mass, in the form of an iron core, moves in proportionally to the applied acceleration within a cylindrical form on which are would three adjacent coils. The entire system is 60 to 70 percent critically damped by immersion in a damping fluid of proper viscosity.

Displacement of the mass is detected by the change in electromagnetic coupling of the coils. The primary coil located at the center, is excited by approximately 2.5 volts RMS at 22.5 RC. The secondaries, on either side, are connected in phase opposition, so that the net output is zero when the core is perfectly centered. Motion of the core increases the voltage induced in the secondary in the direction of motion and reduces the voltage induced in the other secondary. The net output is a voltage which is a linear function of the displacement of the core (within the design range of the instrument); phase depends on the direction of motion, changing 180° as the core passes through the equilibrium position.

Damping is employed to reduce "ringing" of the system after the applied acceleration is removed. Quantitatively it has been shown that 60 to 70 percent of critical damping extends the range of usefulness of the accelerometer to nearly 75 percent of its natural frequency and produces an almost linear phase-lag relation in this range, thereby eliminating phase distortion. It can also be shown that the response of such a damped system to a step function input is within 1 percent of the true value within 5/8 of its natural period. The ensuing oscillations about the true value never exceed 1-1/2 percent and damp out rapidly. Thus, for the type AB-3 accelerometer which was used, the natural period of which is 4 milliseconds (250 cycles/sec), the response to a suddenly applied acceleration of constant magnitude is within 1 percent of the true value in 2.5 milliseconds. The response to accelerations which require some time to reach peak amplitude is closer to the true values.

To separate the intelligence from the 22.5-kc carrier requires a phase discriminator and detector. These functions are performed in the S. Sterling Model 301 Differential Transformer Amplifier. In addition, the driving voltage is obtained from this instrument. Briefly, the excitation voltage is derived from a conventional oscillator-driven amplifier transformer coupled to the accelerometer primary. The secondary outputs are amplified and then applied to a phase-discriminator amplitude detector stage. The output of this stage is a voltage, the amplitude of which is proportional to the acceleration and the polarity of which depends on the direction of acceleration. A four-stage RC low-pass filter is utilized in the output to attenuate the 22.5-kc carrier.

The output of the differential transformer amplifier is applied to the d-c y-axis amplifier of a Du Mont Type 304-H oscillograph through the calibration and pre-amplifier circuit shown schematically in Fig. 19. Here provision is made for selecting the accelerometer signal or an accurately known calibration voltage in the form of a step function. The circuit also permits the insertion of a single-stage resistance-coupled triode pre-amplifier when necessary. The high-frequency response of this pre-amplifier is intentionally attenuated to reduce the 22.5 kc carrier output further without materially affecting the low-frequency components up to approximately 1000 cycles. The d-c response of the entire system is sacrificed in the interest of simplicity by the use of the 1-mf coupling condenser in the output of this circuit. The time constant of this condenser and the 2-megohm input impedance of the oscillograph is 2 seconds. It can easily be shown that the response of such a system to a step function at the end of 0.02 second (a typical sweep time) is only 1 percent below the true value (note the calibration traces, Fig. 15). Response to any other signal will be more accurate.

In obtaining data, a single driven sweep of the oscillograph is employed, and the trace is photographed by a Du Mont Type 297 oscillograph-record camera operating on the Polaroid-Land principle. The sweep is triggered

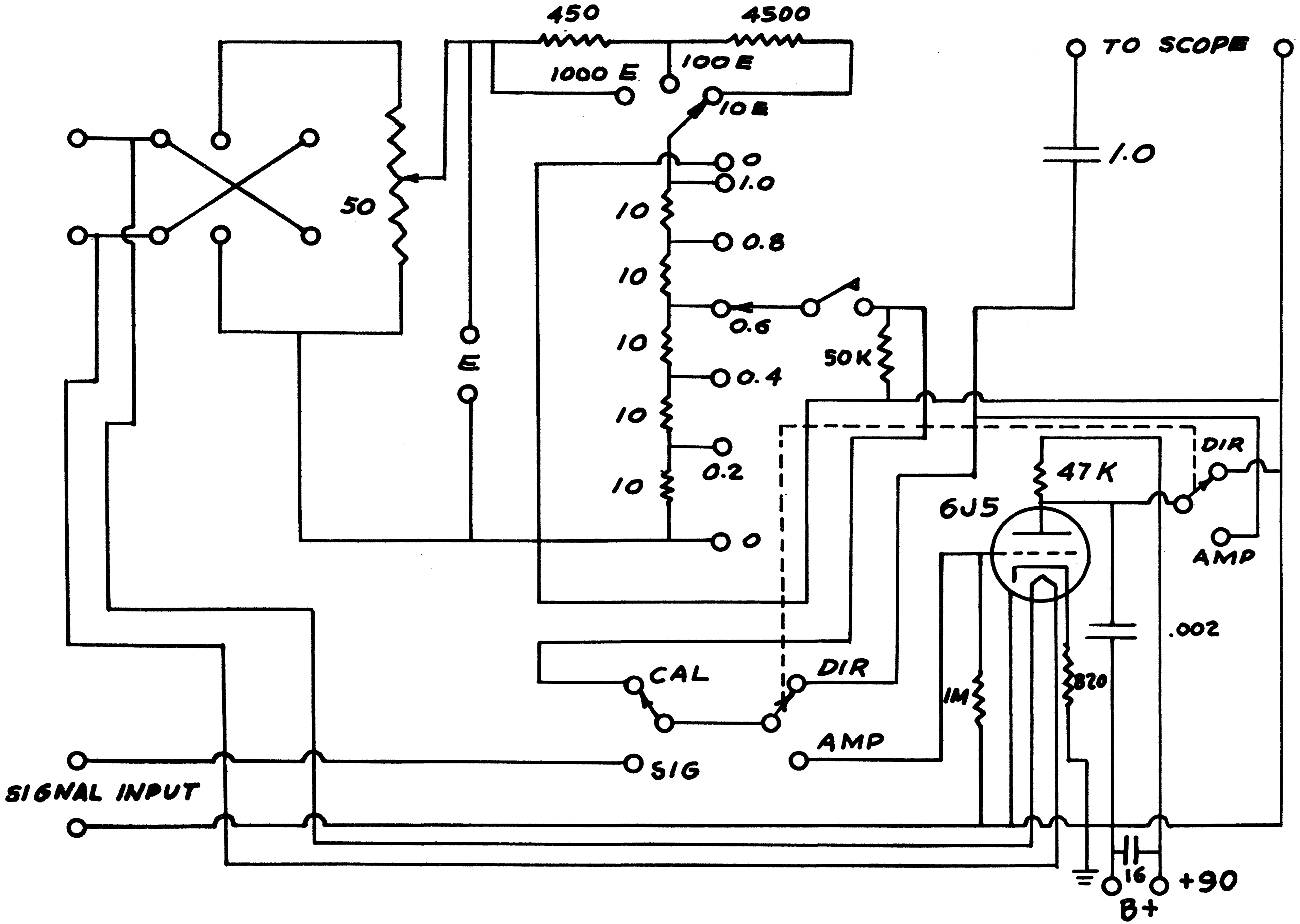

FIG. 19 – CALIBRATION AND PRE-AMPLIFIER CIRCUIT

by a signal obtained by opening the switch which generates the spark for igniting the mixture in the tube. The entire spark system is shielded to eliminate the interference which would otherwise mask the desired signal.

Time calibrations of each trace are obtained by blanking the oscillograph beam with pulses spaced at known time intervals. To produce these pulses, the circuit of Fig. 20 was employed. This circuit is variously known as a cathode-coupled clipper or a slicer. It is essentially an overdriven two-stage RC coupled amplifier with positive feedback introduced by the common cathode resistor. Driven by a calibrated oscillator, its output is a rectangular wave of steep slope synchronized at the oscillator frequency. Differentiating the output produces a series of pulses of alternate polarity. The positive pulses are attenuated by the crystal rectifier across the output. The remaining negative pulses, spaced by the oscillator period, are applied to the z-axis oscillograph input, thereby blanking the beam at a known frequency.

To eliminate the extraneous signals due to microphonics, the entire instrumentation with the exception of the accelerometer, is located about 30 feet from the blast tube. Thus all the events of interest are recorded before the sound waves of the blast reach the equipment to generate microphonic signals.

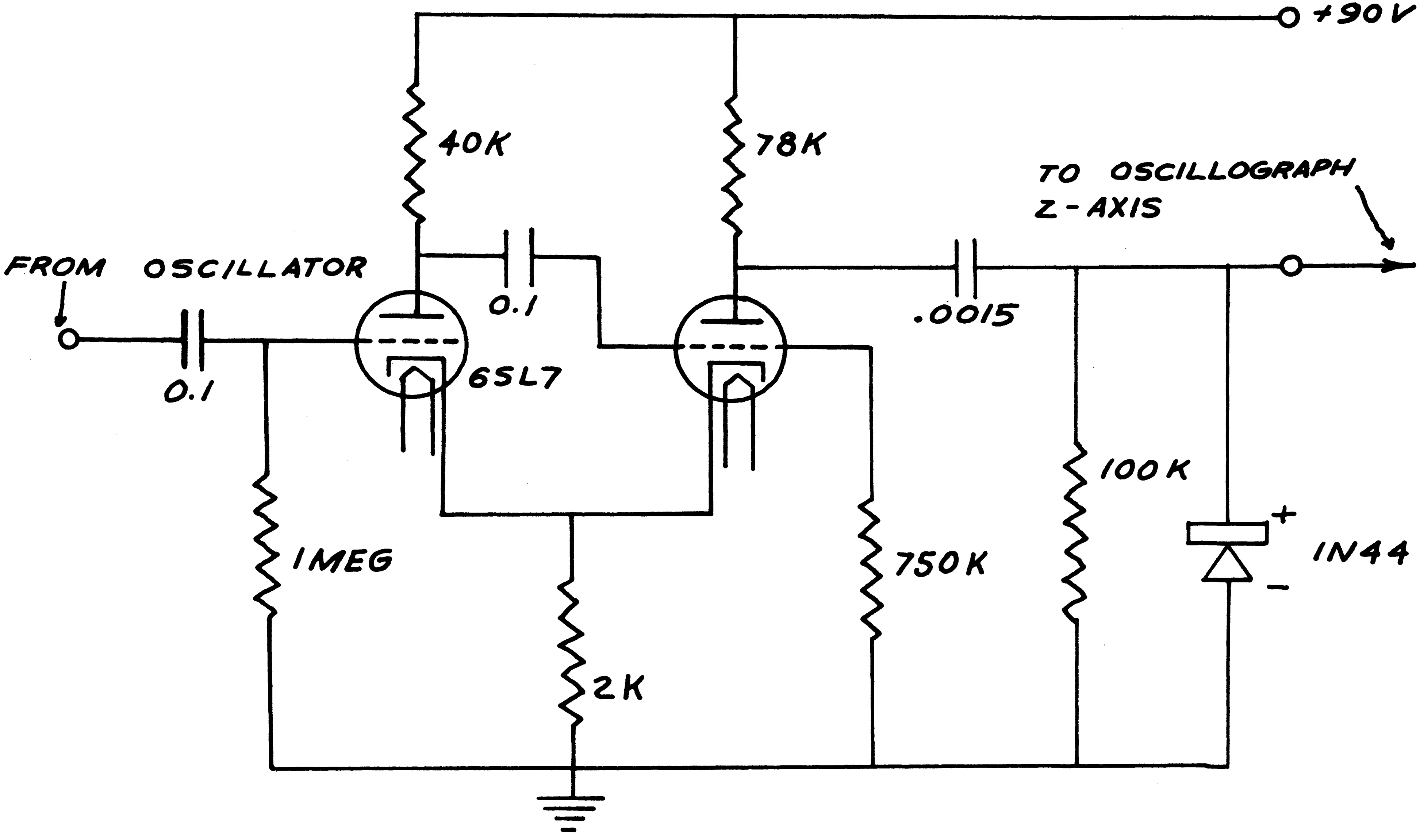

FIG. 20 - BLANKING PULSE GENERATOR

APPENDIX B. CALIBRATION PROCEDURE

To obtain quantitative data from the accelerometer signals, it was necessary to calibrate the output of the differential transformer amplifier in terms of millivolts as a function of the acceleration experienced by the accelerometer. Known accelerations were obtained by the spring-mass system shown schematically in Fig. 21. Here the accelerometer is a portion of a mass suspended on a spring. The entire system is stressed by a known force composed of weight suspended from the accelerometer by means of a fusible link of 0.016-inch piano wire. Electrically melting the link releases the weight, whereupon the mass is accelerated upward by a known force equal to the released weight. The effect of the distributed mass of the spring is taken into account by adding 1/3 of its total mass to that of the suspended mass[5]. This empirical correction is accurate to within 1.5 percent for the case when the suspended mass and that of the spring are equal and the error is reduced for the larger suspended masses employed. The output of the accelerometer and associated instrumentation is recorded by photographing the single driven sweep of the oscillograph. Triggering of the sweep is accomplished by a signal obtained from the same switch which closes the electric circuit to melt the fusible link.

Following each recording of an accelerometer signal, a calibration grid composed of step-function voltages of known values is superimposed on the picture. Thus a calibration in terms of millivolts per g acceleration is obtained (see Fig. 22). By superimposing a similar calibration grid on subsequent detonation tube records, quantitative information of the values of recorded accelerations is obtained.

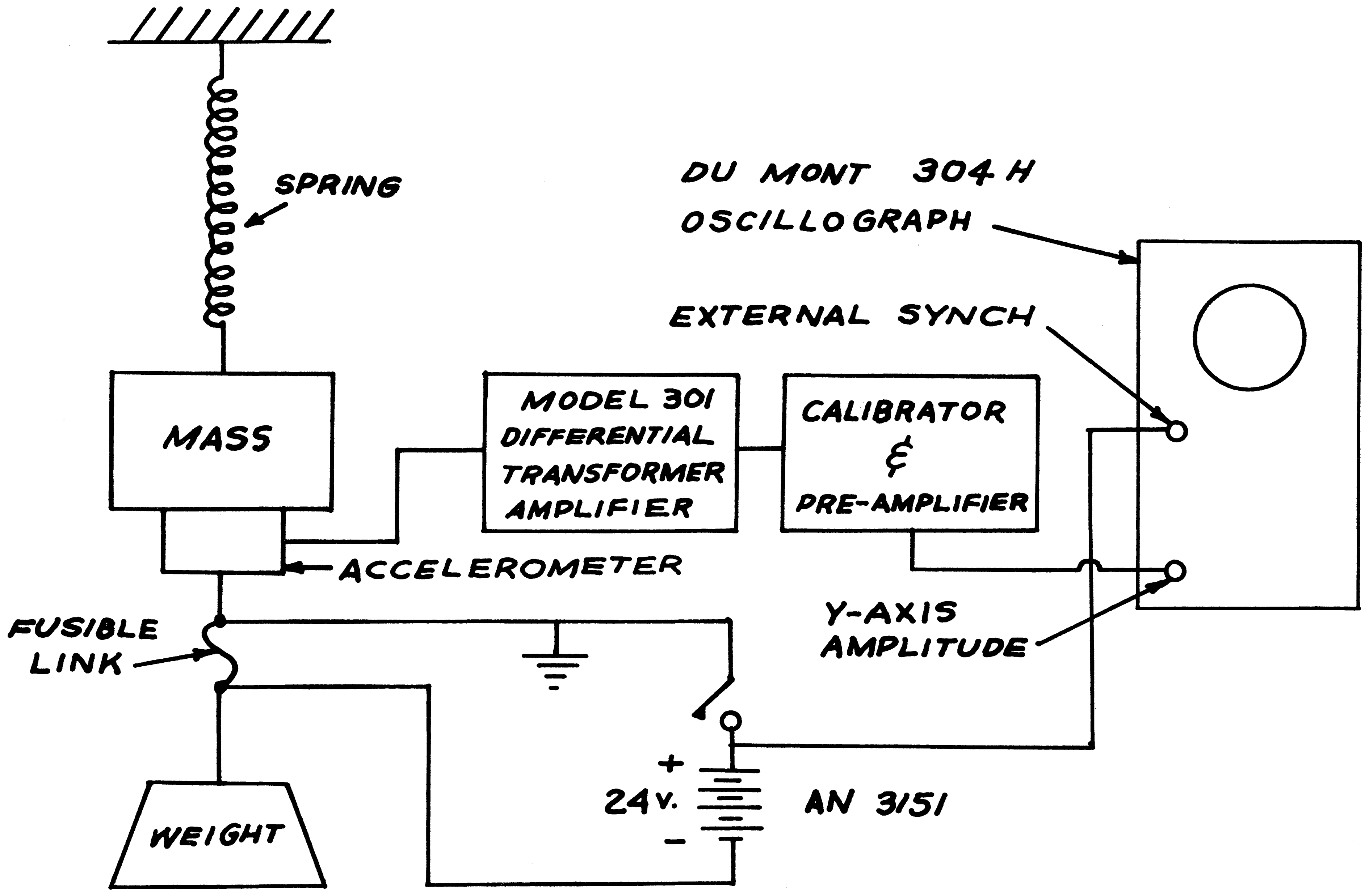

FIG. 21 – SCHEMATIC OF ACCELEROMETER CALIBRATION

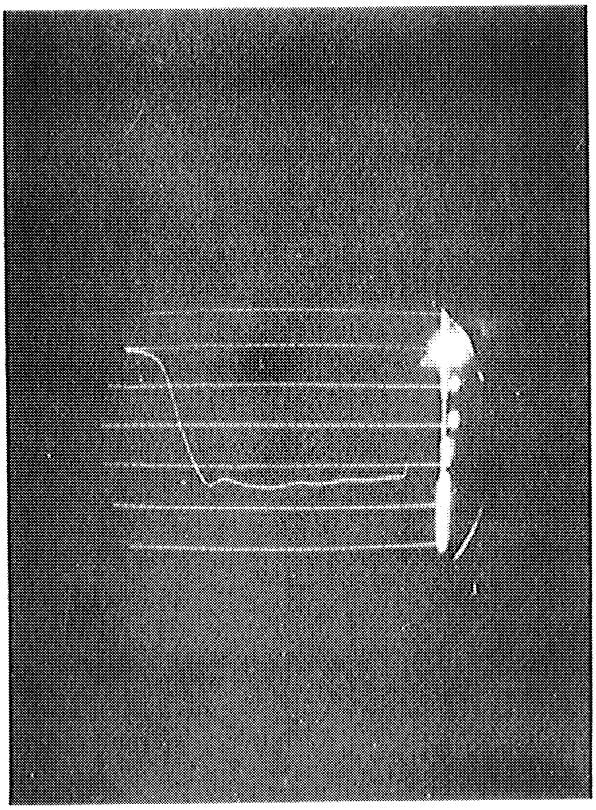

Fig. 22. Typical Accelerometer Calibration Run.

REFERENCES

1. Morrison, R. B., Nicholls, J. A., and Ong, R., "Preliminary Calculations on the Thrust and Impulse Characteristics of Intermittent Detonation," University of Michigan Engineering Research Institute, not yet published.

2. Morrison, R. B., "A Shock Tube Investigation of Detonative Combustion," Report UMM-97, University of Michigan, Engineering Research Institute, January, 1952.

3. Nicholls, J. A., Morrison, R. B., Reid, F. A., and Ong, R., "Final Report on Detonative Combustion," Project M898, University of Michigan, Engineering Research Institute, August, 1953.

4. Weir, A. Jr., and Morrison, R. B., "Equilibrium Temperatures and Compositions behind a Detonation Wave," Paper presented before Division of Gas and Fuel Chemistry, 124th Meeting, ACS, Chicago, Ill., September, 1953.

5. Myklestad, N. O., Vibration Analysis, McGraw-Hill, New York, 1944.